Steel and Composite Structures, *Vol. 19, No. 1 (2015) 237-262*
DOI: http://dx.doi.org/10.12989/scs.2015.19.1.237

Probabilistic sensitivity analysis of multi-span highway bridges

M. Bayat [1], F. Daneshjoo [*1] and N. Nisticò [2]

[1] *Department of Civil and Environmental Engineering, Tarbiat Modares University, Tehran, Iran*
[2] *Department of Structural and Geotechnical Engineering, Università degli Studi di Roma "La Sapienza", Roma, Italy*

(*Received December 11, 2014, Revised February 15, 2015, Accepted April 29, 2015*)

Abstract. In this study, we try to compare different intensity measures for evaluating nonlinear response of bridge structure. This paper presents seismic analytic fragility of a three-span concrete girder highway bridge. A complete detail of bridge modeling parameters and also its verification has been presented. Fragility function considers the relationship of intensities of the ground motion and probability of exceeding certain state of damage. Incremental dynamic analysis (IDA) has been subjected to the bridge from medium to strong ground motions. A suite of 20 earthquake ground motions with different range of PGAs are used in nonlinear dynamic analysis of the bridge. Complete sensitive analyses have been done on the response of bridge and also efficiency and practically of them are studied to obtain a proficient intensity measure for these types of structure by considering its sensitivity to the period of the bridge. Three dimensional finite element (FE) model of the bridge is developed and analyzed. The numerical results show that the bridge response is very sensitive to the earthquake ground motions when PGA and Sa (Ti, 5%) are used as intensity measure (IM) and also indicated that the failure probability of the bridge system is dominated by the bridge piers.

Keywords: highway bridge; fragility curve; nonlinear time history analysis; finite element modeling

1. Introduction

Seismic vulnerability and seismic performance of highway bridges have became an important subject especially after the 1971 San Fernando earthquake because of damages during the large excitations. In the straight bridges the superstructure centerline is perpendicular to the sub-structural elements and the responses of longitudinal and transverse directions have a little coupling. Fragility curves represent the relationship between the ground motion intensities and the probability of exceeding certain state of damage. Fragility curves respect to their base and aims of their developing, following two important targets. First designers can use these curves to examine the effect of changing different design parameters on structure's behavior and predict the extent of probable damages, and the second programmers can use the curves to increase their reliability in decision making and planning.

Fragility curves can be divided into two categories:

*Corresponding author, Professor, E-mail: danesh_fa@modares.ac.ir

http://www.techno-press.org/?journal=scs&subpage=8 ISSN: 1229-9367 (Print), 1598-6233 (Online)

(a) Empirical fragility curves which are drawn on the basis of information obtained in the previous earthquake damages.
(b) Analytical fragility curves which are produced by numerical simulation of the seismic response of structures using dynamic analysis of structures.

The most reliable analysis method is the full-time history analysis but mostly due its excessive complexity engineers and designers tend to prefer simpler methods such as nonlinear static analysis.

Analytical Fragility curves are useful tools to predict the extent of damages. These curves calculate the behavior of the structure and damages as a function of earthquake parameters. Generating fragility curves and evaluating the performance using the analytical method requires the use of a series of earthquakes. Many studies have been conducted considering variety of scenarios.

First approach: In some studies, a large number of natural or synthetic accelerograms are selected with regard to the structure and seismicity of the region and the analysis of probabilistic seismic is done in order to produce the needed models. In this method there's a cloud of information that exists in $M_w - R$ space. This method of producing fragility curves is called cloud approach.

Second approach: In this approach a series of earthquakes are selected and analysis is achieved to extract the fragility curves, using a small set of earthquakes, magnitude of earthquake is scaled and increased step by step. This method is called Incremental Dynamic Analysis (IDA).

One of the most advantages of Incremental Dynamic Analysis (IDA) is that, we can consider the behavior of the structure from initial elastic response until global dynamic instability will occur. The second advantages of this approach is that by considering a suit complete records, we can find the seismic fragility of the structure analytically with the consideration of different states of structure.

Empirical fragility curves were developed for California bridges by Basöz and Kiremidjian in (1999). Yamazaki *et al*. (2000) and Shinozuka *et al* (2000a) tried to achieve a set of empirical fragility curves based on the actual damage date due to the Kobe earthquake. Mander and Basöz (1998) and Hwang and Huo (1998), generated analytical fragility curves of bridge from their seismic response against actual earthquake data.

Shinozuka *et al*. (2000b) studied on the usage of a simplified nonlinear analysis method (nonlinear static procedure) to develop fragility of the structure, but they indicated that this method don't show constant agreement with nonlinear time history analysis in terms of predicting all levels of damage. Many other scientists have been worked on developing probabilistic analysis in structural engineering in open literatures (Cimerallo *et al*. 2010, Mackie *et al*. 2010, Wright et a. 2011, Padgett *et al*. 2010, Ramanathan 2012, Pan *et al*. 2010, Banerjee and Shinozuka 2008, Eads *et al*. 2013, Sung and Su 2011, Tavares *et al*. 2012, Deepu *et al*. 2014, Kameshwar and Padgett 2014, Karim and Yamazaki 2003, Kaviani 2011, Monti and Nistico 2002, Monti *et al*. 2001).

In this study, incremental dynamic analysis is used to develop seismic fragility functions of the bridge. Developing analytical fragility curves consist of simulation of ground motions, modeling of bridges, and developing fragility curves from response results of analysis. The response of the structure is obtained by applying incremental dynamic analysis which is the most accurate method.

The main objective of this research is to consider different spectral intensity measures and PGA and the response sensitivity to them and assess the vulnerability of a three-span simply supported

concrete girder highway bridges when subjected to medium to strong earthquakes. Efficiency and practically of the used intensity measures to achieve a proficient intensity measure of this type of bridges is also presented and compared. A detailed three dimensional model of the bridge has been presented and its seismic analytical fragility curves are developed based on the results of incremental dynamic analysis. A full nonlinear time history analysis are utilized to evaluate the seismic response of bridge components (bridge piers) and individual component fragility functions derived from the incremental dynamic analysis results are combined to evaluate the overall fragility of the bridge system.

2. Bridge modeling and verification

2.1 Modeling description

The model used in this study is derived from a non-skewed model developed by Nielson (2005), the characteristics of which are based on data obtained from a survey of numerous bridge plans. The common type of the bridge throughout the Central and South-eastern United States is concrete slab on concrete girder highway bridges accounting for approximately 40% of all highway bridges in the region. A typical bridge configuration with standard details is derived through the data collection of concrete girder bridges (Nielson 2005). Figs. 1 and 2 show typical scheme of a Multi-

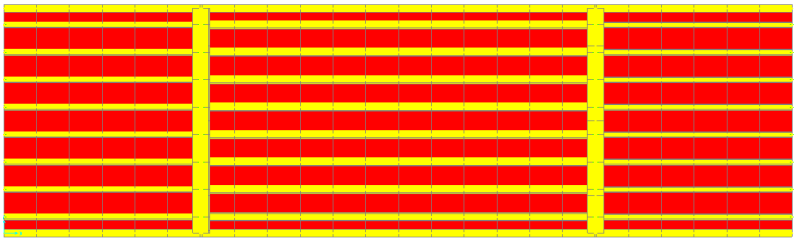

Fig. 1 Bridge deck modeling (Extruded)

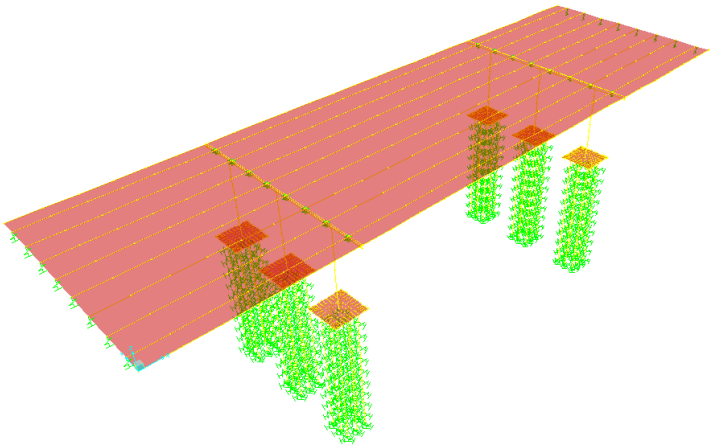

Fig. 2 Three dimensional model of the bridge in SAP2000 (Without extruding)

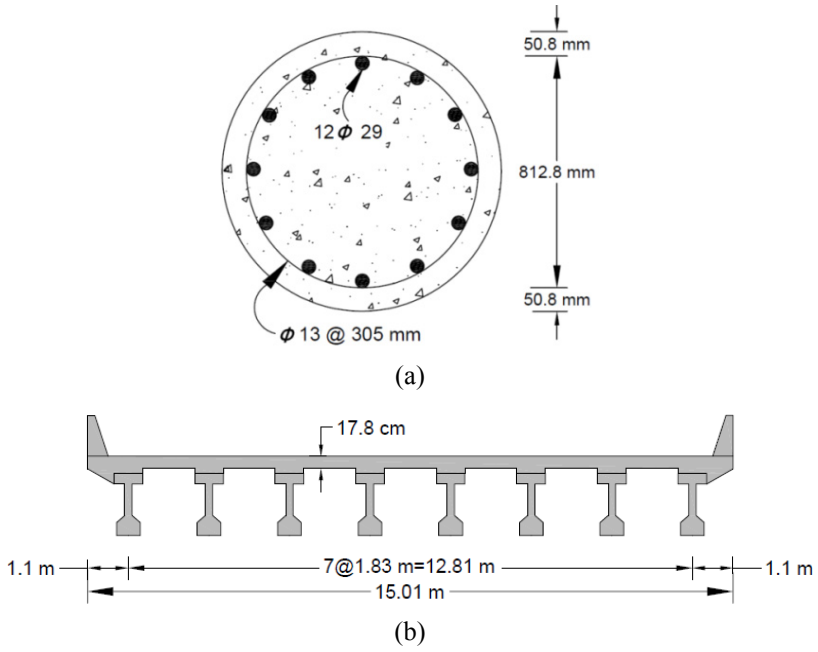

Fig. 3 Concrete member reinforcing layout: (a) column; (b) deck detail

Span Simply Supported Concrete (MSSS Concrete) girder bridge. Total length of the bridge is 48.8 m and its three spans have 12.2-24.4 and 12.2 m length. The width of bridge is 15.01 m with eight AASHTO type prestressed girders. AASHTO Type I and III girders are used for the end and centre spans. Elastomeric pads are the bearing of this bridge. The pads for end spans are 406 mm long by 152 mm wide and 25.4 mm thick and for the centre span are 559 mm long by 203 mm wide and still 25.4 mm thick. The details of columns, bridge deck and piles are shown in Figs. 3 and 4. The concrete strength at the design procedure is assumed to be 20.7 MPa while the yield strength of reinforcing steel is 414 MPa. More detailed specifications of these columns are in an investigation of existing bridge plans and also from the work done by Hwang *et al*. (2001). The pile caps are 2438 mm square and 1092 mm thick. The pile cap is connected with the columns using 914 mm long lap splices at the bases of the columns. The abutments used for this bridge are the pile-bent girder seat type abutments.

The software used has different nonlinear link elements to model plastic elements, bearings and etc. For each deformation degree of freedom we can capture the nonlinear force deformation relationship with a nonlinear link element. The deck is modelled using shell elements. Bilinear plastic model are used to model the place of plastic hinges. The places of plastic hinges are at the bottom segments of the columns. The abutments are modelled using beam elements supported on springs. A rigid bar is used to connect the nodes between girders and bearings, bearings and cap beams, and cap beams and tops of the columns. Abutments and the column boundary conditions are fixed-free in the longitudinal direction and fixed-fixed in the transverse direction. In the longitudinal direction each columns acts as a vertical cantilever beam therefore the longitudinal motion of the bridge is the most critical response which could cause damage to bridge components. The plastic hinges in the typical bridges are form at bottom of the columns.

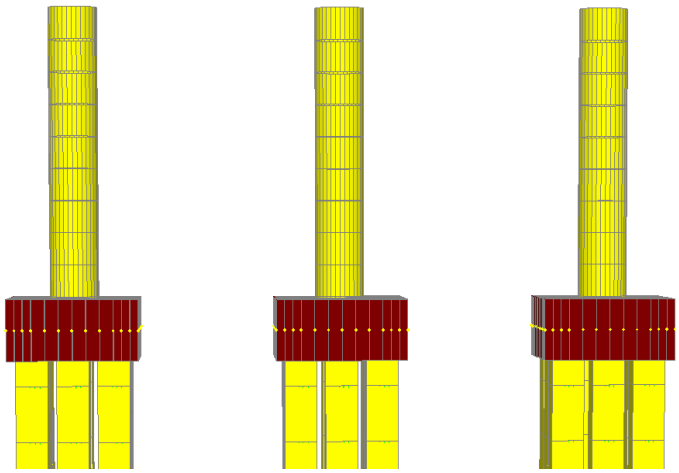

Fig. 4 Scheme of columns and pile foundation modeling in SAP2000

The curvature for each column section ϕ_y can be obtained from Eq. (1)

$$\phi_y = \frac{M_n}{M_y}\phi'_y \tag{1}$$

M_n is moment corresponding to a compressive strain of ε = 0.005, M_y is the moment at first yielding of a vertical reinforcing bar and ϕ'_y is the curvature at first yielding of a vertical reinforcing bar.

The length of the plastic hinge is obtained from

$$L_p = 0.08L + 0.022 f_y d_{bl} \geq 0.044 f_y d_{bl} \quad (f_y \text{ in MPa}) \tag{2}$$

L = length from the point of contraflexture to the section

d_{bl} = diameter of a longitudinal reinforcing bar

To define the nonlinear behaviour of the bilinear plastic link elements at the base of columns the moment-rotation relationship are used as input.

The bearings are elastomeric pads and their behaviour are modelled with an elastic–perfectly plastic material. The bearings of center spans have an initial stiffness of 6.2 kN/mm and the end spans have an initial stiffness of 3.4 kN/mm. Lateral pile stiffnesses were assumed at 7 kN/mm/pile (Nielson 2005) and the vertical stiffnesses were assumed to be 175 kN/mm/pile (Nielson 2005).

2.2 Seismic response and verifications

A single synthetic ground motion specific to Memphis, TN, from the suite of Rix ground motions (Rix and Fernandez-Leon 2004) is used to obtain the seismic response of the bridge. The duration of the earthquake record is 25.1 seconds with the magnitude of it is 7.5 R with epicentre distance of 20 km. Acceleration time history of Rix ground motion with a peak ground acceleration (PGA) of 0.65 g is shown in Fig. 5 and its response spectrum with 5% damping is

shown in Fig. 6. Time steps of 0.0025 seconds are chosen in the time history analysis. The ground motion is applied at the pile caps and abutments where the soil-structure interaction is simply accounted for with a set of springs. The modelling procedure is verified by comparing the results with Nielson model (Nielson 2005) as presented in Table 1.

The first period of the bridge model is 0.59 in the longitudinal direction. The second mode is a transverse mode with a period of 0.48 seconds. For the nonlinear time history analysis we ignore the effects of soil-structure interaction, therefore the period of the bridge is 0.55s.

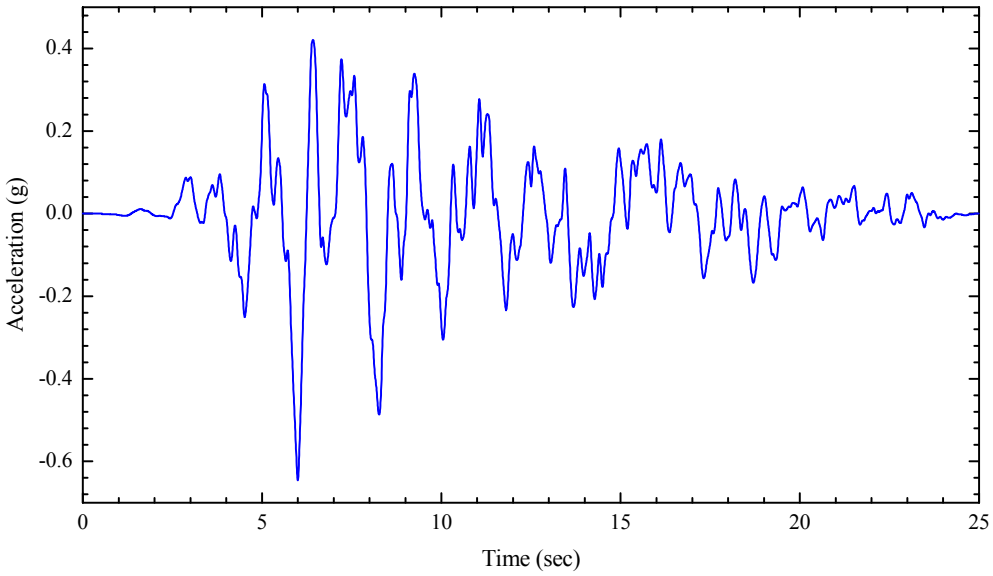

Fig. 5 Time history of ground motion used for illustration of seismic responses (Nielson 2005)

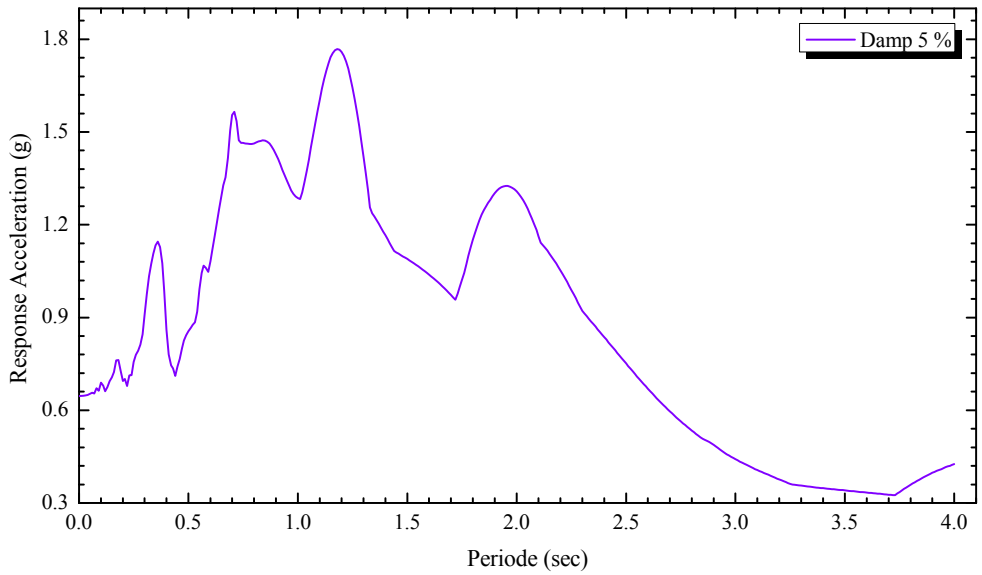

Fig. 6 Response spectrum (5% damping) of ground motion used for illustration of seismic (Nielson 2005)

Table 1 Comparisons of the results of present study and reference (Nielson 2005)

Comparative responses	Nielson (2005)	Present study	Differences	Verified results
First period	0.62 s	0.59 s	0.04	verified
Second period	0.46 s	0.48 s	0.04	verified
Maximum displacement of the deck	100 mm	96 mm	0.04	verified

3. Seismic ground motion records

A relationship is needed between the ground motion records as our input and structural damage as our output to have a comparison between them.

It is very important how to select the models of the bridges and also the input ground motions. When a nonlinear time history is applied to a structure, all the nonlinearity of the members is take into account. It is obvious that the responses of the bridges are subsequently dependent on the characteristics of earthquake ground motions. Therefore the frequency content and intensity and the ground type have a great effect on the response of the bridges. A reasonable intensity measure and a structural damage can lead us to a good correlation.

Many different intensity measure factors are used to describe the severity of the earthquake ground motion such as: PGA, peak ground velocity (PGV), peak ground displacement (PGD), time duration of strong motion (Td), spectrum intensity (SI) and etc. In this study, PGA, Sa (T1, 5%) and a range of Sa (0.05T1, 5%) to Sa (2.5T1, 5%) are used as intensity measure factors.

Table 2 Characteristics of the earthquake ground motion histories (FEMA 2003)

	Earthquake				Recording station	
ID No.	M	PGA	Year	Name	Name	owner
1	7.0	0.48	1992	Cape Mendocino	Rio Dell Overpass	USGS
2	7.6	0.21	1999	Chi-Chi, Taiwan	CHY101	CWB
3	7.1	0.82	1999	Duzce,Turkey	Bolu	ERD
4	6.5	0.45	1976	Friuli, Italy	Tolmezzo	----------
5	7.1	0.35	1999	Hector Mine	Hector	SCSN
6	6.5	0.34	1979	Imperial Valley	Delt	UNAMUCSD
7	6.5	0.35	1979	Imperial Valley	El Centro Array#1	USGS
8	6.9	0.38	1995	Kobe, Japan	Nishi-Akashi	CUE
9	6.9	0.51	1995	Kobe,Japan	Shin-Osaka	CUE
10	7.5	0.24	1999	Kokaeli,Turkey	Duzce	ERD
11	7.3	0.36	1992	Landers	Yemo Fire Station	CDMG
12	7.3	0.24	1992	Landers	Coolwater	SCE
13	6.9	0.42	1989	Loma Prieta	Capitola	CDMG
17	6.7	0.44	1994	Northridge	Canyon Country-WLC	USC
18	6.6	0.36	1971	San Ferando	LA-Hollywood Stor	CDMG
19	6.5	0.51	1987	Superstition Hills	El Centro Imp.Co	CDMG
20	6.5	0.52	1987	Superstition Hills	Poe Road (temp)	USGS

Table 2 shows some information of 20 earthquake ground motion records with different range of PGA form medium to strong motions which are used to perform incremental dynamic analysis (IDA).

Fig. 7 shows the acceleration response spectra with 5% damping ratio of the selected recorded ground motions. The average diagram of the selected records is shown in bold line.

Fig. 8 represents the different percentiles of acceleration response spectra with 5% damping ratio. From Fig. 8 is indicated that that the selected records contain medium to strong ground motions. Figs. 9 (a) and (b) are the PGA and PGV variations of the selected records.

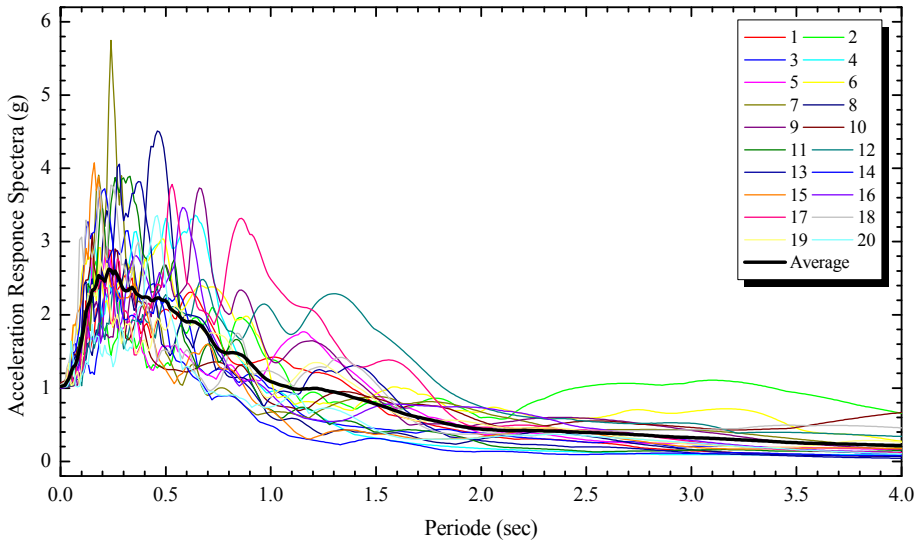

Fig. 7 Response acceleration spectra of far field ground motions

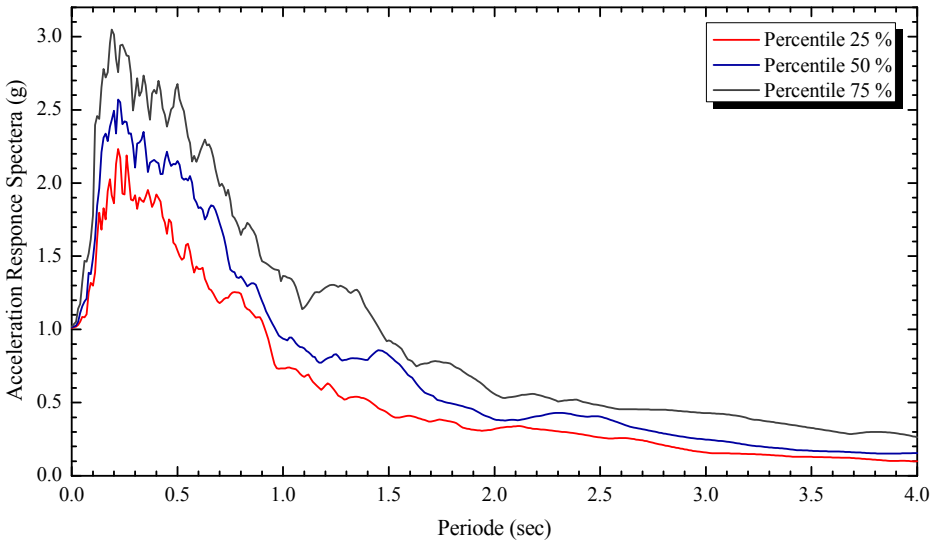

Fig. 8 Percentiles of response acceleration spectra of a suit of 20 far field earthquake ground motion records

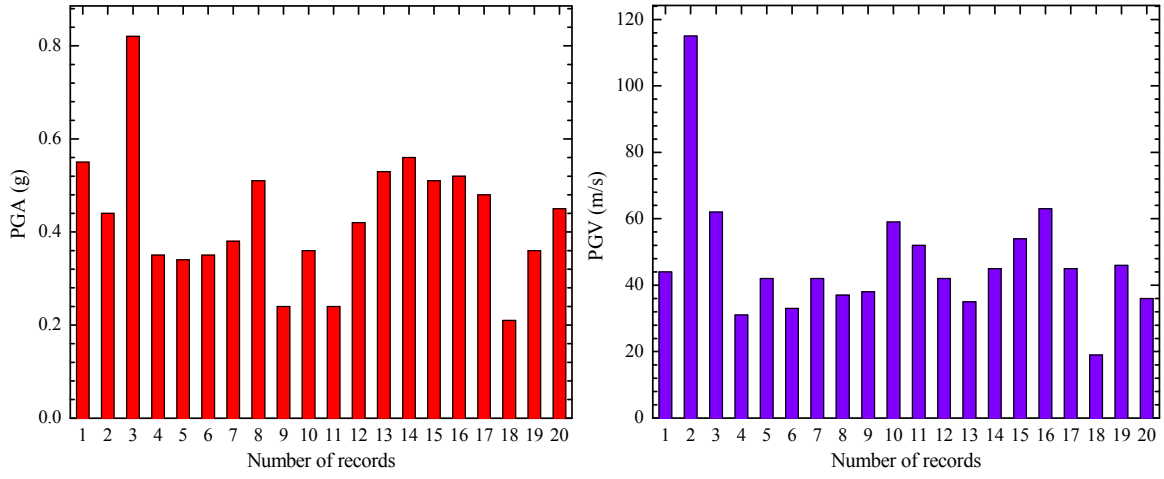

Fig. 9 (a) Variation of PGA respect to the number of the records; (b) variation of PGV respect to the number of the records

4. Incremental Dynamic Analysis (IDA)

One of the methods which have been considered by the researchers in the field of performance-base earthquake engineering is incremental dynamic analysis (IDA). This method is able to prepare valuable information about the seismic demand and capacity, estimating the response of structure by increasing the intensity level of ground motion and predict the probability of reaching or exceeding specific damage states for a given level of peak earthquake intensities (represented here by PGA and Sa (Ti, 5%) for different periods). To apply the incremental dynamic analysis to the bridge, we should have a proper nonlinear structural model for our first step. Then a suite of records (at least 20) are compiled and scaled to different intensity levels with the increment of 0.1 (FEMA 2003). For each record the dynamic analysis run and the results post-processed. Total nonlinear analyses are more than 500. We can generate IDA curves of the structural response with a damage measure and intensity measure.

4.1 Fragility curves and intensity measures

Fragility curves were formulated by the work presented by Cornell *et al*. (2002) condition upon an Intensity Measure (IM) by suing incremental dynamic analysis. The fragility curves are the relation between the seismic hazard and response of structures and modeled as lognormal distribution (Cornell *et al*. 2002)

$$P\left[D \geq d \middle| IM\right] = 1 - \Phi\left(\frac{\ln(d) - \ln(S_d)}{\beta_{D|IM}}\right) \tag{3}$$

$\phi(\bullet)$ = Standard normal cumulative distribution function
S_D = Median value of the structural demand in terms of a seismic intensity
$\beta_{D|IM}$ = Logarithmic standard deviation, or dispersion, of the demand conditioned on the IM.

The relation between SD and IM estimated as

$$S_D = aIM^b \tag{4}$$

With a linear regression we can obtain the coefficient of a and b and re-written the Eq. (5) as

$$\ln(SD) = b.\ln(IM) + \ln(a) \tag{5}$$

The dispersion of the mean demand conditioned on the IM is

$$\beta_{D|IM} \cong \sqrt{\frac{\sum(\ln(d_i) - \ln(b.\ln(IM) + \ln(a)))^2}{N-2}} \tag{6}$$

N = number of ground motions
di = Peak demands

4.2 Efficient intensity measure

If an IM is efficient it should have a less dispersion about the median of the results of nonlinear time history analysis. $\beta_{D|IM}$ is the dispersion of the results around the median of the response in this study. The lower values of $\beta_{D|IM}$ leads to a more efficient intensity measure Padgett *et al*. (2008).

4.3 Practical intensity measure

Padgett *et al*. (2008) presented a new criteria for selecting an optimal intensity measure in bridges. They introduce the practically of an intensity measure which is the relation between the dependency of the structural response and seismic hazard. They identified the practically as a coefficient of the regression parameter b in Eq. (5). The higher value of b leads to a more practical intensity measure in comparison together.

4.4 Proficient intensity measure

Padgett *et al*. (2008) composite the measure of efficiency and practically as new criteria of selecting an optimal intensity measure as follow formulation

$$P\left[D \geq d \middle| IM\right] = 1 - \Phi\left(\frac{\ln(IM) - \frac{\ln(d) - \ln(a)}{b}}{\frac{\beta_{D|IM}}{b}}\right) \tag{7}$$

A lower values of modified dispersion is a more proficient IM

$$\zeta = \frac{\beta_{D|IM}}{b} \tag{8}$$

A complete procedure of developing analytical fragility curves is shown in the following algorithm in Fig. 10.

4.5 Limit states of the nonlinear time history analysis

A suitable engineering demand parameter (EDP) of bridge which has a great correlation to the intensity measure (IM) leads to less dispersion in the results. In the conventional highway bridges the piers columns are the most critical component in the bridges and they always have a nonlinear behavior under strong ground motions (Yi *et al*. 2007).

FEMA-356 has defined three important limit states for concrete reinforcement columns such as: Immediate Occupancy (IO), Life Safety (LS), Collapse Prevention (CP). Table 3 represent the Numerical Acceptance Criteria for Nonlinear Procedures — Reinforced Concrete Columns.

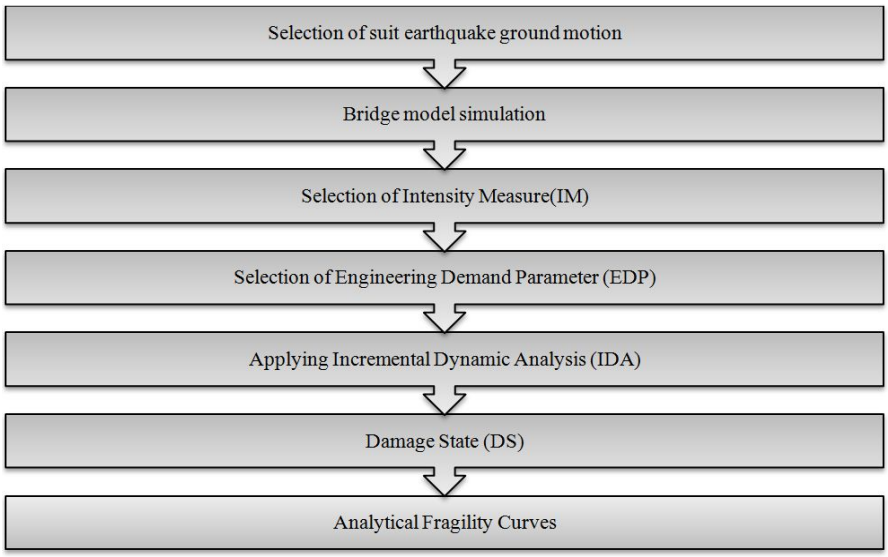

Fig. 10 Methodology of generating analytical fragility curves

Table 3 Numerical Acceptance Criteria for Nonlinear Procedures— Reinforced Concrete Columns

Conditions			Acceptance criteria				
			LO	LS	CP	LS	CP
Columns controlled by flexure							
$\frac{p}{A_g f_c'}$	Trans Reinf	$\frac{v}{b_w d\sqrt{f_c'}}$					
≤ 0.1	C	≤ 3	0.005	0.015	0.02	0.02	0.03
≤ 0.1	C	≥ 6	0.005	0.012	0.016	0.016	0.024
≥ 0.4	C	≤ 3	0.003	0.012	0.015	0.018	0.025
≥ 0.4	C	≥ 6	0.003	0.01	0.012	0.013	0.02
≤ 0.1	NC	≤ 3	0.005	0.005	0.006	0.01	0.015
≤ 0.1	NC	≥ 6	0.005	0.004	0.005	0.008	0.012
≥ 0.4	NC	≤ 3	0.002	0.002	0.003	0.006	0.01
≥ 0.4	NC	≥ 6	0.002	0.002	0.002	0.005	0.008

5. Results and discussions

In this section we consider different intensity measures related to their sensitivity on the period of the bridge and we consider the efficiency and practically of them and finally the proficiency. Figs. 11 and 12 are shown the Incremental dynamic analysis curves for PGA and Sa (T1, 5%) as intensity measures. All the analysis was done till collapse prevention of the bridge is appeared. It has been observed from the figures that the bridge behavior is started from the elastic range till the inelastic range by increasing the steps of the nonlinear time history analysis. The IDA curves are

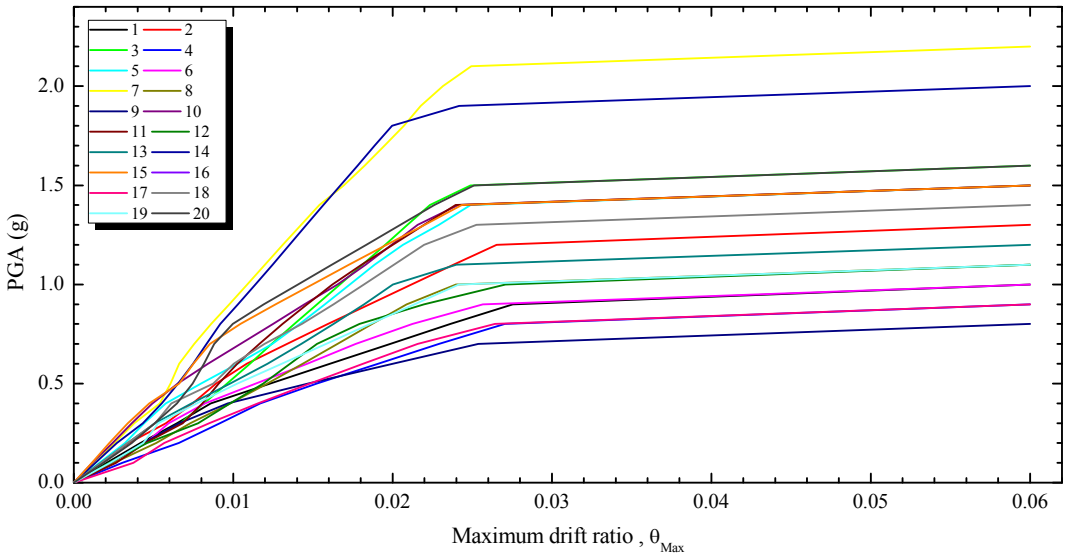

Fig. 11 All twenty IDA curves: IM = PGA, EDP = θ_{max}

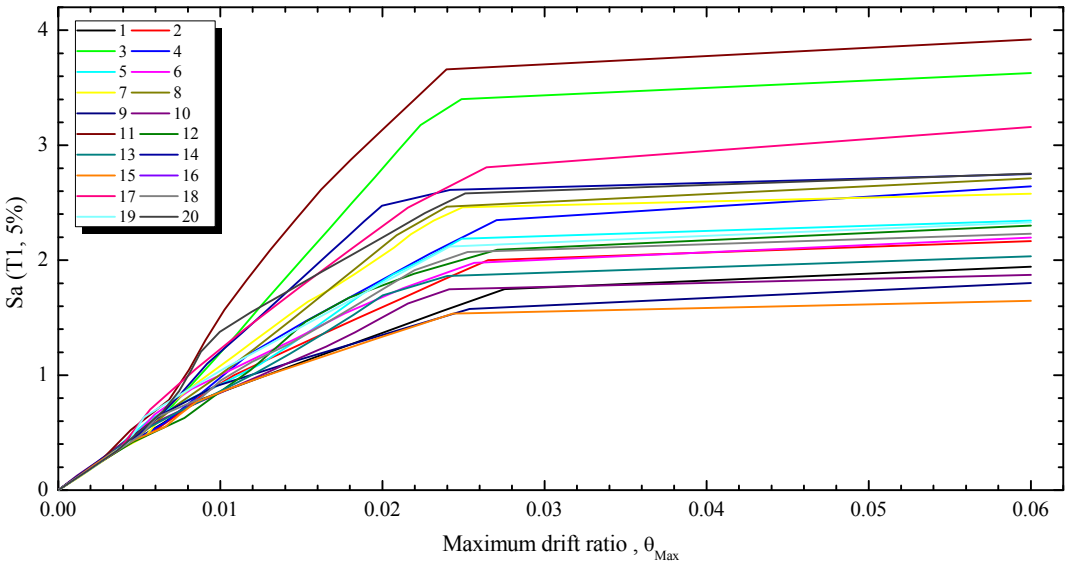

Fig. 12 All twenty IDA curves : IM = Sa (T1, 5%), EDP = θ_{max}

derived for column drift ratio as engineering demand parameter (EDP) to have a better understanding from the behavior of the critical component of the bridges.
We have done more than 500 nonlinear time history analysis and the data are used in log-normal distribution and we have obtained the dispersion from $\beta_{D|IM}$ in Eq.(5) which is presented the efficiency of the intensity measures. The results of dispersion for different values of Sa (Ti, 5%) respect to different structural period are shown in Table 4. From this comparison we have figured out that the Sa (1.1T1, 5%) and Sa (1.2T1, 5%) are more efficient than the other spectral intensity measures, because of their lower $\beta_{D|IM}$ values.

Table 4 Comparisons of regression values of PGA and Sa (T1, 5%) and dispersion values

IM	*a*	*b*	$\beta_{D\|IM}$	$\zeta = \frac{\beta_{D\|IM}}{b}$
PGA(g)	0.009	0.893	2.5866	2.8966
Sa (0.05T1, 5%)	0.017	0.913	1.1142	1.2204
Sa (0.1T1, 5%)	0.014	0.833	1.2208	1.4655
Sa (0.2T1, 5%)	0.011	0.731	1.6950	2.3187
Sa (0.3T1, 5%)	0.009	0.730	1.8398	2.5203
Sa (0.4T1, 5%)	0.008	0.807	1.6750	2.0756
Sa (0.5T1, 5%)	0.008	0.821	1.5082	1.8370
Sa (0.6T1, 5%)	0.009	0.859	1.5149	1.7635
Sa (0.7T1, 5%)	0.009	0.848	1.2725	1.5006
Sa (0.8T1, 5%)	0.009	0.837	1.2772	1.5260
Sa (0.9T1, 5%)	0.009	0.867	1.2877	1.4852
Sa (T1, 5%)	0.010	0.952	1.1559	1.2142
Sa (1.1T1, 5%)	**0.011**	**0.981**	**0.6822**	**0.6954**
Sa (1.2 T1, 5%)	**0.012**	**0.969**	**0.6543**	**0.6753**
Sa (1.3T1, 5%)	0.012	0.954	0.8142	0.8534
Sa (1.4T1, 5%)	0.014	0.985	0.8855	0.8989
Sa (1.5T1, 5%)	0.014	0.939	0.7188	0.7655
Sa (1.6T1, 5%)	0.014	0.920	0.8977	0.9757
Sa (1.7T1, 5%)	0.016	0.909	1.0085	1.1094
Sa (1.8T1, 5%)	0.018	0.866	1.0390	1.1998
Sa (1.9T1, 5%)	0.018	0.830	1.1218	1.3516
Sa (2T1, 5%)	0.019	0.798	1.2372	1.5504
Sa (2.1T1, 5%)	0.034	0.742	2.6823	3.6150
Sa (2.2T1, 5%)	0.018	0.691	1.4438	2.0894
Sa (2.3T1, 5%)	0.018	0.673	1.5729	2.3372
Sa (2.4T1, 5%)	0.019	0.671	1.6475	2.4553
Sa (2.5T1, 5%)	0.019	0.686	1.6780	2.4460

To consider the practically of an intensity measure we should find the correlation between the intensity measures and the engineering demand parameters (EDP) in the log-normal space.
Collecting all the data of nonlinear time history analysis, the coefficients (a and b) of the linear regression analysis have been evaluated.

Regression R squared and b show the correlations between the IM and EDP in logarithmic space: the value of b, shows the practically of the intensity measures (Padgett *et al.* 2008). Finally, the "Proficient" composite intensity measure ($\beta_{D|IM}/b$)is evaluated*:* alower value of the modified dispersion is correlated to a more proficient IM.

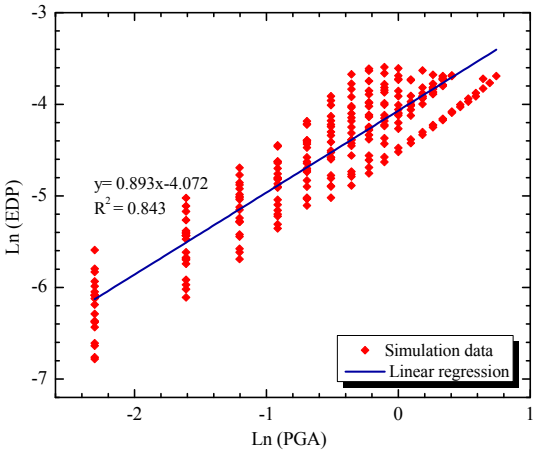

Fig. 13 Simulated maximum column drift ratio (as EDP) of bridge as a function of PGA (as IM) of earthquake motions

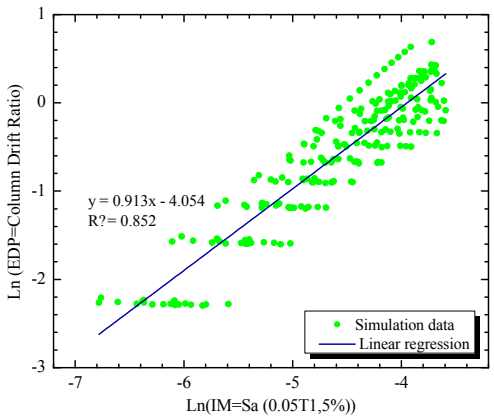

Fig. 14 Simulated maximum column drift ratio (as EDP) of bridge as a function of Sa (0.05T1, 5%) (as IM) of earthquake motions

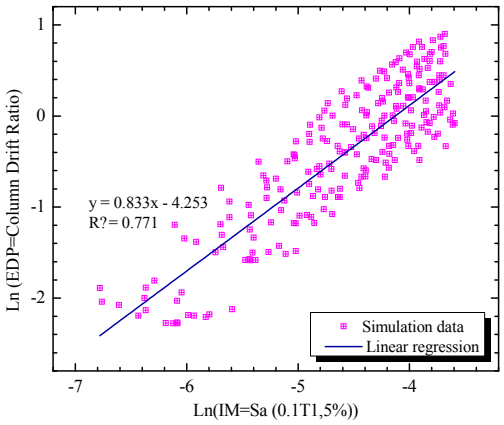

Fig. 15 Simulated maximum column drift ratio (as EDP) of bridge as a function of Sa (0.1T1, 5%) (as IM) of earthquake motions

From the comparison of the proficiency of the different intensity measure, we have obtained that Sa (1.2T1, 5%) is more proficient than the other spectral intensity measures,and that we have a critical range of the intensity measures which results are more sensitive. This range is Sa (T1, 5%) to Sa (1.7T1, 5%). It means that if we use spectral intensity measures we should find the critical range of the intensity measure which would prepare less dispersion and more practical and proficient in the results.

Figs. 13 to 39 show the results of linear regression of different intensity measures.

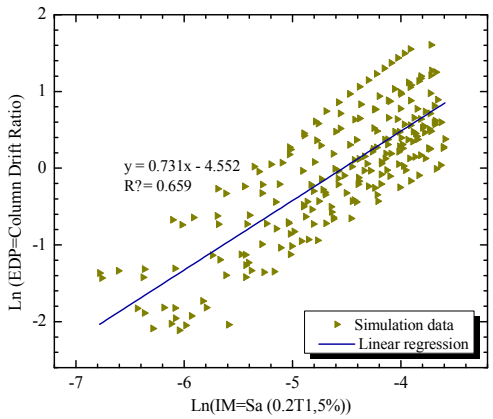

Fig. 16 Simulated maximum column drift ratio (as EDP) of bridge as a function of Sa (0.2, 5%) (as IM) of earthquake motionsd

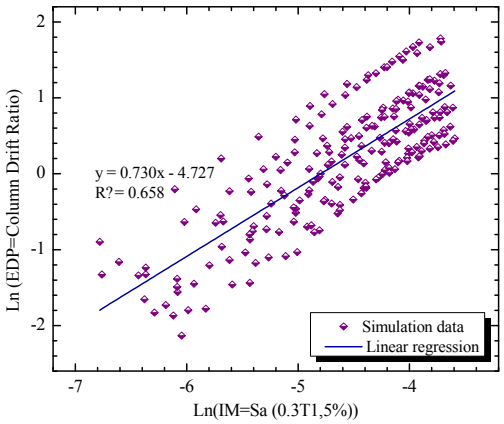

Fig. 17 Simulated maximum column drift ratio (as EDP) of bridge as a function of Sa (0.3T1, 5%) (as IM) of earthquake motions

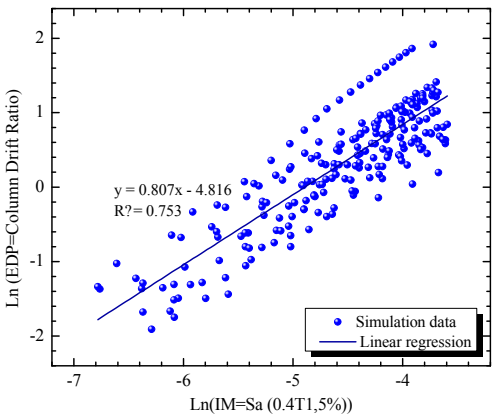

Fig. 18 Simulated maximum column drift ratio (as EDP) of bridge as a function of Sa (0.4T1, 5%) (as IM) of earthquake motions

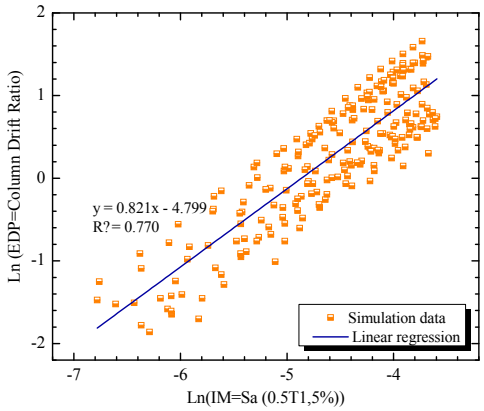

Fig. 19 Simulated maximum column drift ratio (as EDP) of bridge as a function of Sa (0.5T1, 5%) (as IM) of earthquake motions

To full fill our probabilistic task we developed fragility curves of the bridge for different performance level (IO, LS, and CP) (FEMA 2003). The analytical fragility curves show the failure probability of the bridge for a certain values intensity measure. It is strongly suggested to consider other important intensity measures to find the suitable IM which has the less dispersion. To better understand the distribution of data we have presented the 16%, 50% and 84% percentile of PGA for our IDA curves. A high gap between these percentiles shows that the dispersion of data is also high.

Fragility curves for PGA and different spectral intensity measures are developed in Figs. 41 to 68 to show that the dispersion of the results has a great effect on the estimation of the failure probability of the bridge: the dispersion decrease allows more trustable fragility curves.

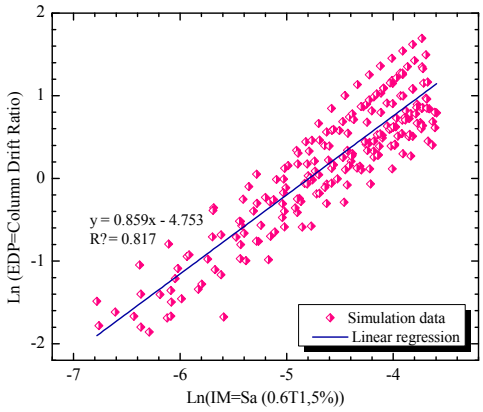

Fig. 20 Simulated maximum column drift ratio (as EDP) of bridge as a function of Sa (0.6T1, 5%) (as IM) of earthquake motions

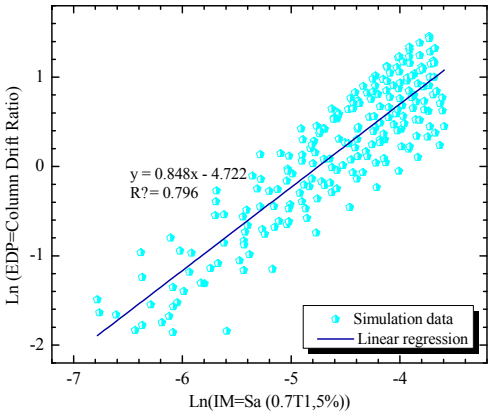

Fig. 21 Simulated maximum column drift ratio (as EDP) of bridge as a function of Sa (0.7T1, 5%) (as IM) of earthquake motions

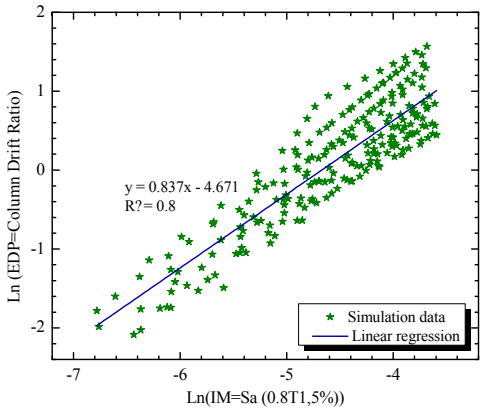

Fig. 22 Simulated maximum column drift ratio (as EDP) of bridge as a function of Sa (0.8T1, 5%) (as IM) of earthquake motions

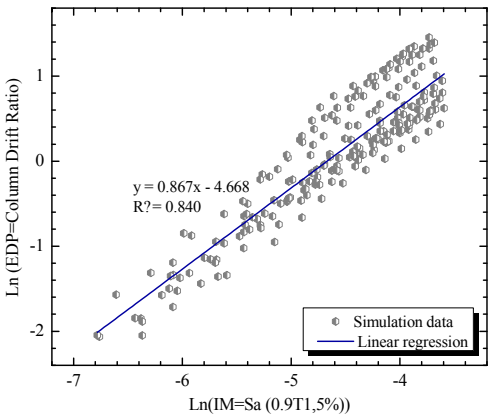

Fig. 23 Simulated maximum column drift ratio (as EDP) of bridge as a function of Sa (0.9T1, 5%) (as IM) of earthquake motions

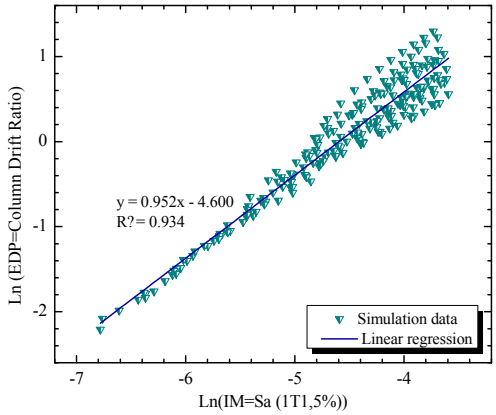

Fig. 24 Simulated maximum column drift ratio (as EDP) of bridge as a function of Sa (T1, 5%) (as IM) of earthquake motions

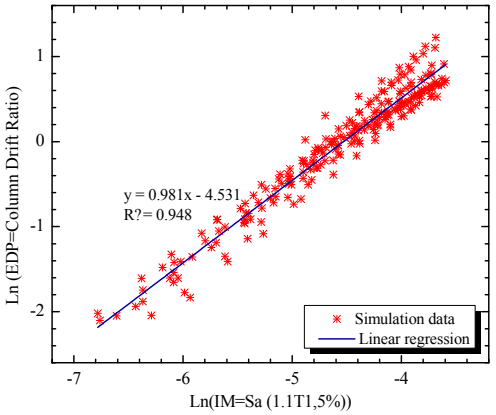

Fig. 25 Simulated maximum column drift ratio (as EDP) of bridge as a function of Sa (1.1T1, 5%) (as IM) of earthquake motions

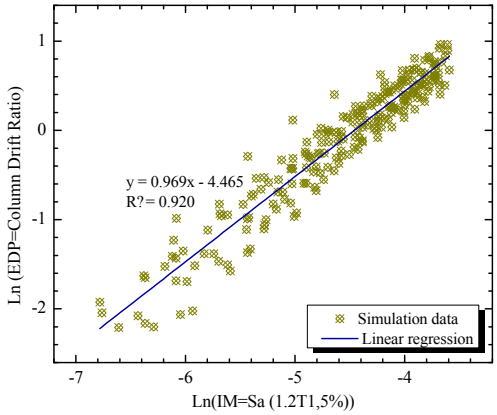

Fig. 26 Simulated maximum column drift ratio (as EDP) of bridge as a function of Sa (1.2T1, 5%) (as IM) of earthquake motions

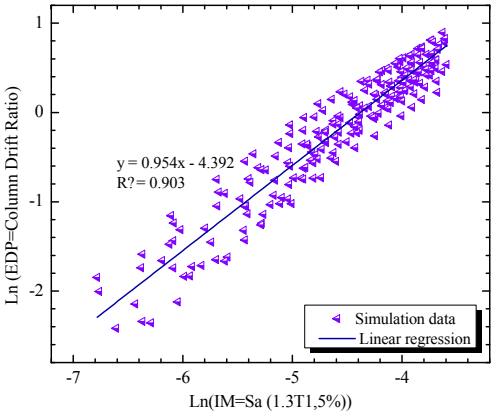

Fig. 27 Simulated maximum column drift ratio (as EDP) of bridge as a function of Sa (1.3T1, 5%) (as IM) of earthquake motions

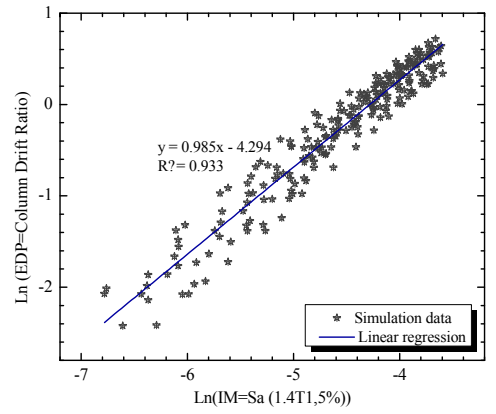

Fig. 28 Simulated maximum column drift ratio (as EDP) of bridge as a function of Sa (1.4T1, 5%) (as IM) of earthquake motions

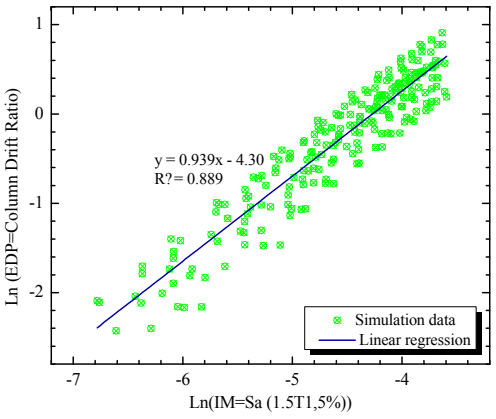

Fig. 29 Simulated maximum column drift ratio (as EDP) of bridge as a function of Sa (1.5T1, 5%) (as IM) of earthquake motions

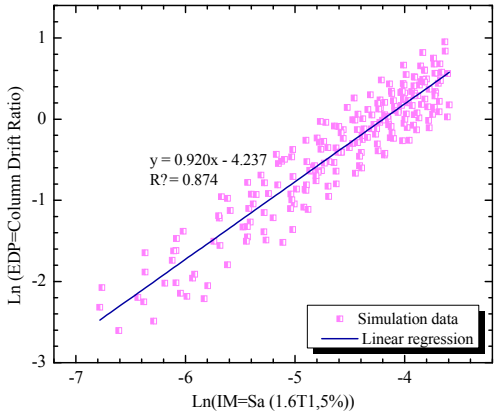

Fig. 30 Simulated maximum column drift ratio (as EDP) of bridge as a function of P Sa (1.6T1, 5%) (as IM) of earthquake motions

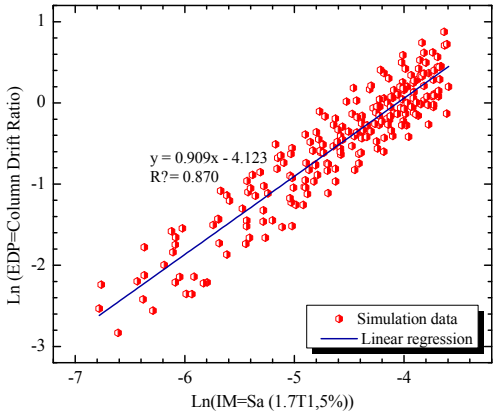

Fig. 31 Simulated maximum column drift ratio (as EDP) of bridge as a function of Sa (1.7T1, 5%) (as IM) of earthquake motions

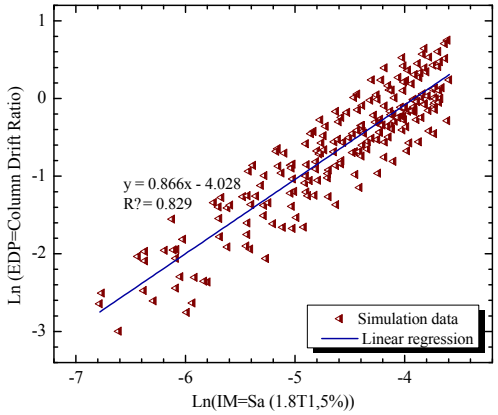

Fig. 32 Simulated maximum column drift ratio (as EDP) of bridge as a function of Sa (1.8T1, 5%) (as IM) of earthquake motions

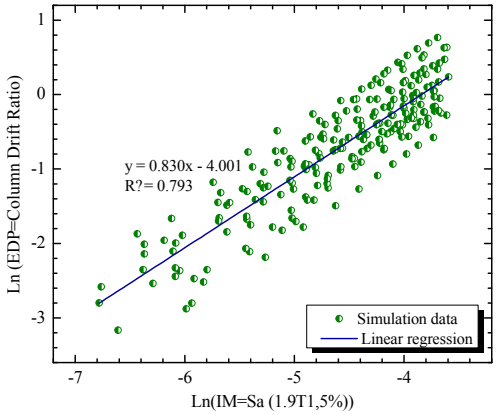

Fig. 33 Simulated maximum column drift ratio (as EDP) of bridge as a function of Sa (1.9T1, 5%) (as IM) of earthquake motions

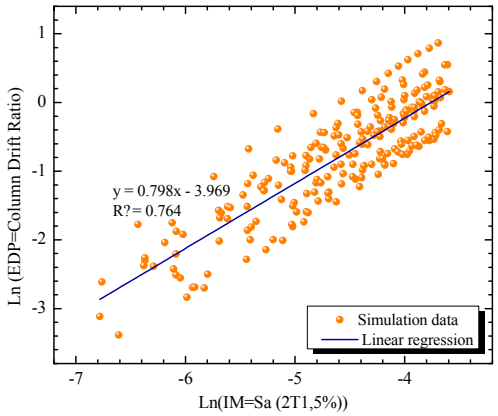

Fig. 34 Simulated maximum column drift ratio (as EDP) of bridge as a function of Sa (2 T1, 5%) (as IM) of earthquake motions

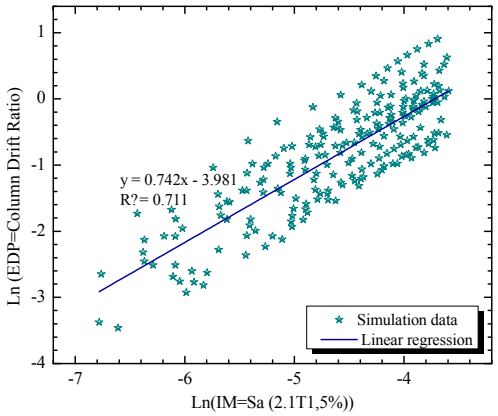

Fig. 35 Simulated maximum column drift ratio (as EDP) of bridge as a function of Sa (2.1T1, 5%) (as IM) of earthquake motions

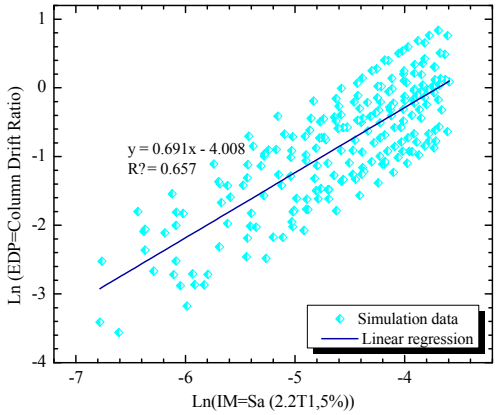

Fig. 36 Simulated maximum column drift ratio (as EDP) of bridge as a function of Sa (2.2T1, 5%) (as IM) of earthquake motions

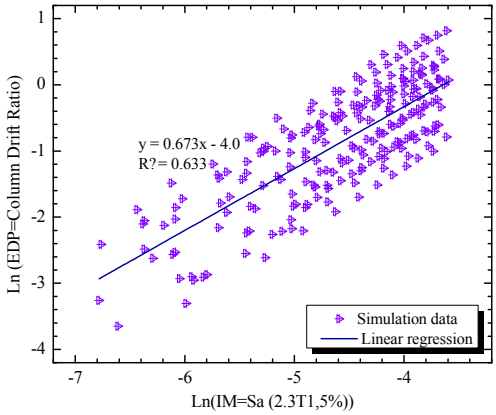

Fig. 37 Simulated maximum column drift ratio (as EDP) of bridge as a function of Sa (2.3T1, 5%) (as IM) of earthquake motions

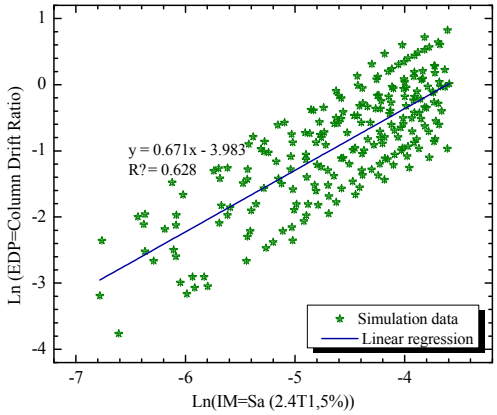

Fig. 38 Simulated maximum column drift ratio (as EDP) of bridge as a function of Sa (2.4T1, 5%) (as IM) of earthquake motions

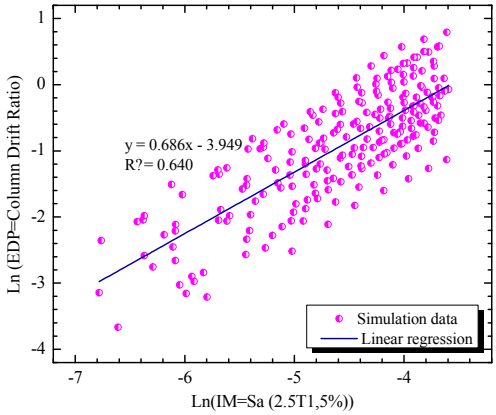

Fig. 39 Simulated maximum column drift ratio (as EDP) of bridge as a function of Sa (2.5T1, 5%) (as IM) of earthquake motions

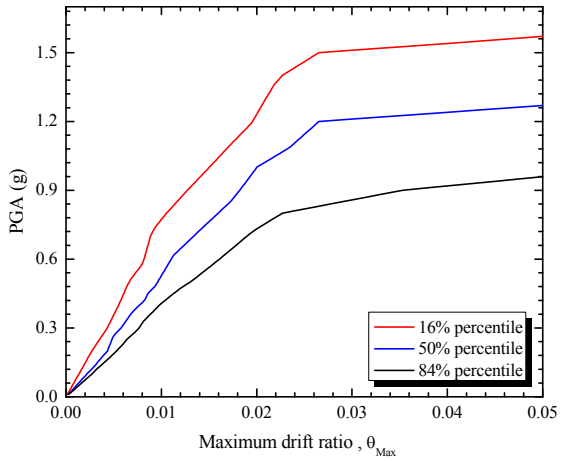

Fig. 40 The summary of the IDA curves into their 16%, 50% and 84% fractal curves of PGA

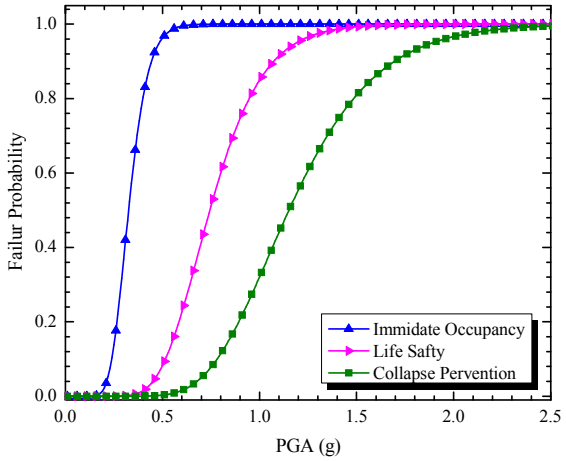

Fig. 41 Fragility curves of the bridge pier respect to PGA

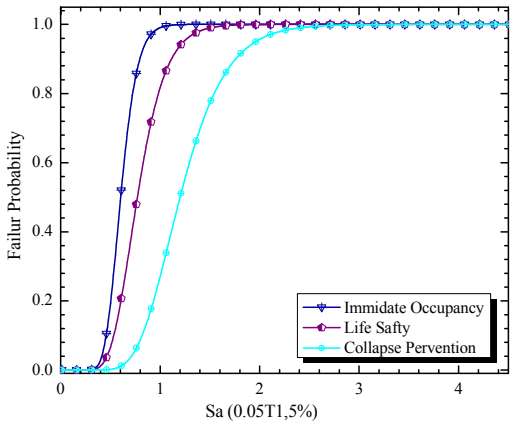

Fig. 42 Fragility curves of the bridge pier respect to Sa (0.05 T1, 5%)

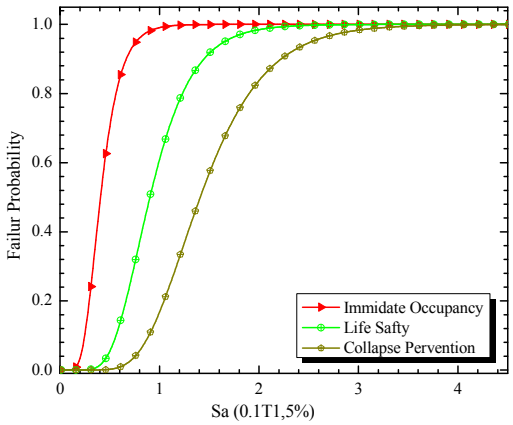

Fig. 43 Fragility curves of the bridge pier respect to Sa (0.1 T1, 5%)

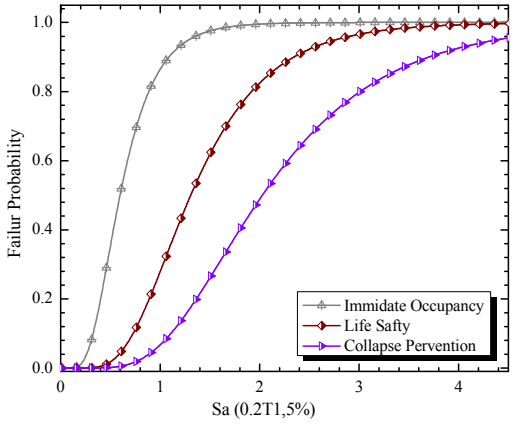

Fig. 44 Fragility curves of the bridge pier respect to Sa (0.2T1, 5%)

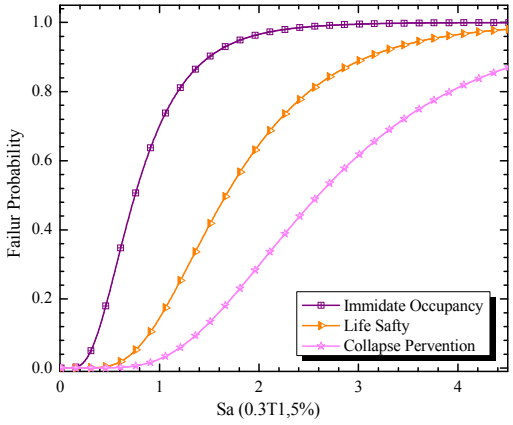

Fig. 45 Fragility curves of the bridge pier respect to Sa (0.3 T1, 5%)

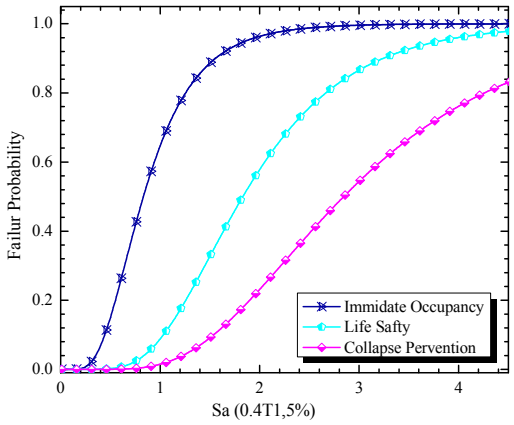

Fig. 46 Fragility curves of the bridge pier respect to Sa (0.4 T1, 5%)

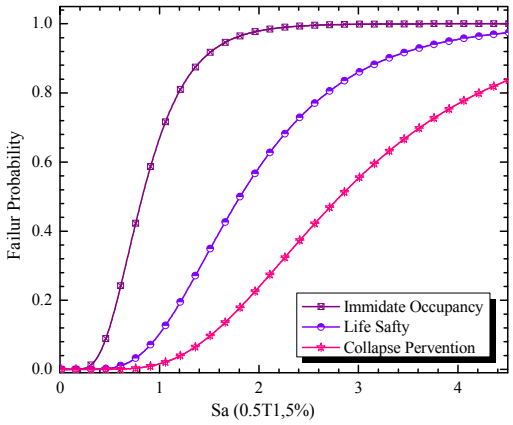

Fig. 47 Fragility curves of the bridge pier respect to Sa (0. 5 T1, 5%)

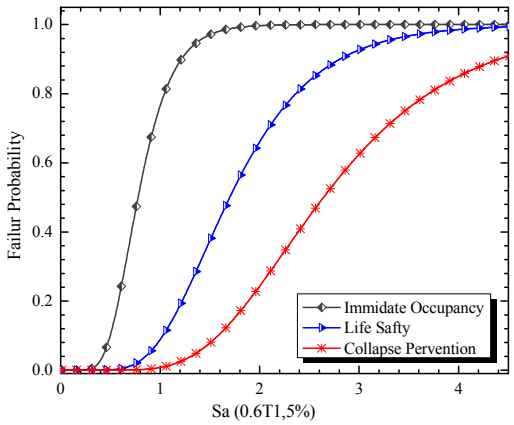

Fig. 48 Fragility curves of the bridge pier respect to Sa (0.6 T1, 5%)

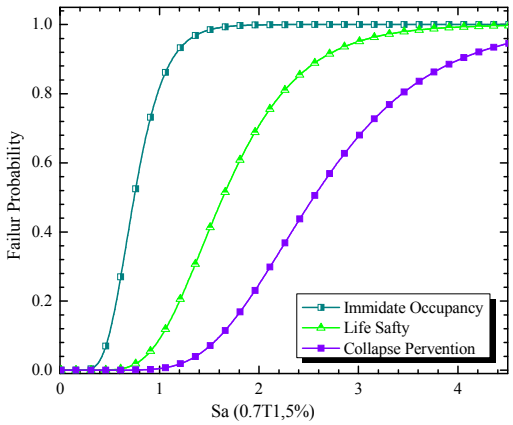

Fig. 49 Fragility curves of the bridge pier respect to Sa (0.7 T1, 5%)

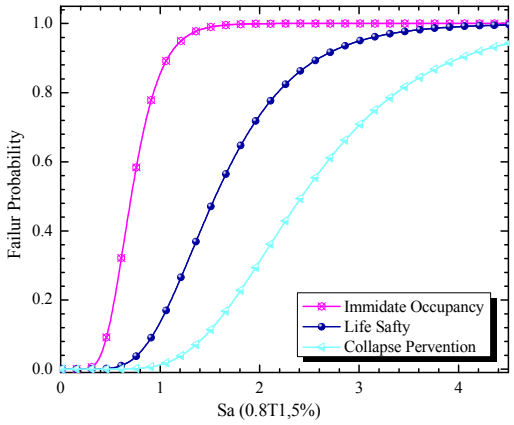

Fig. 50 Fragility curves of the bridge pier respect to Sa (0.8 T1, 5%)

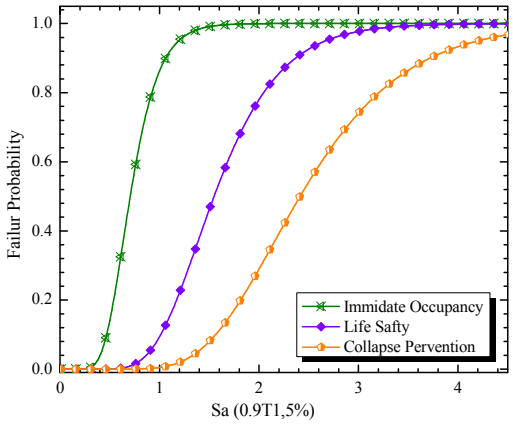

Fig. 51 Fragility curves of the bridge pier respect to Sa (0.9 T1, 5%)

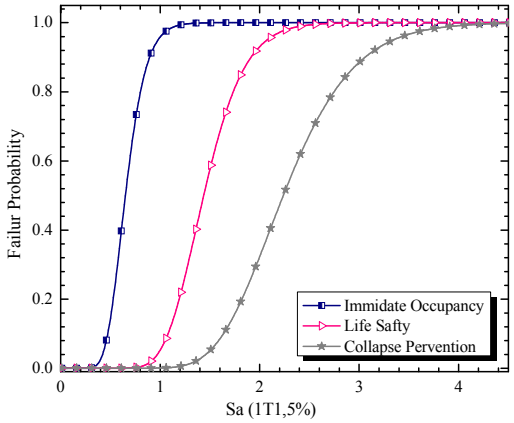

Fig. 52 Fragility curves of the bridge pier respect to Sa (T1, 5%)

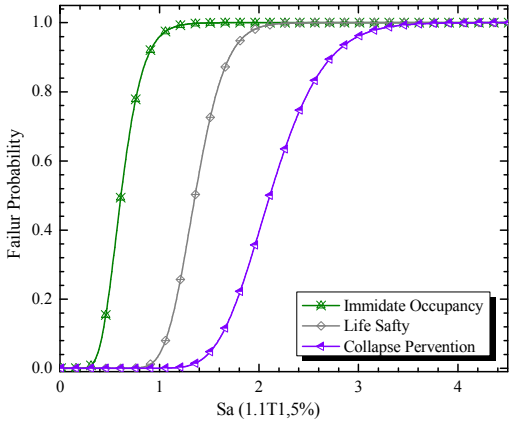

Fig. 53 Fragility curves of the bridge pier respect to Sa (1.1 T1, 5%)

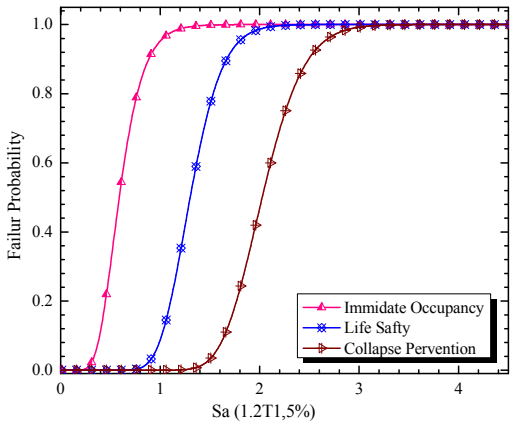

Fig. 54 lity curves of the bridge pier respect to Sa (1.2 T1, 5%)

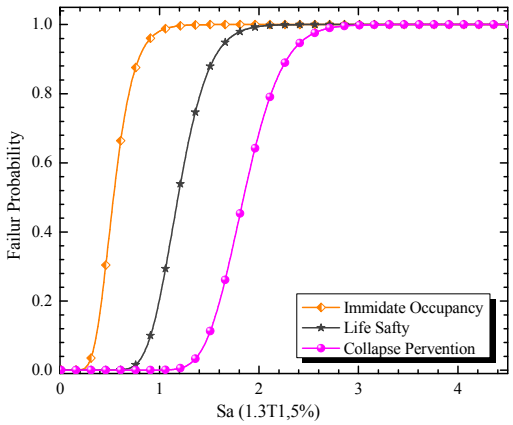

Fig. 55 Fragility curves of the bridge pier respect to Sa (1.3 T1, 5%)

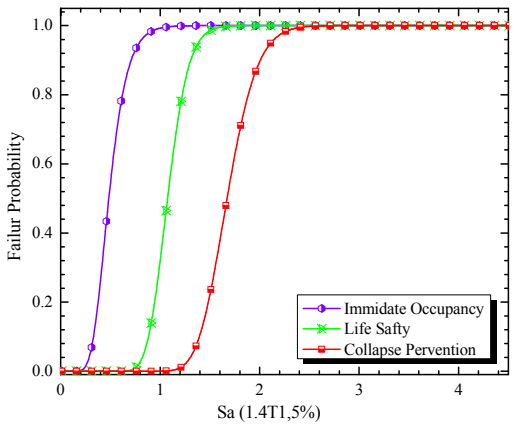

Fig. 56 Fragility curves of the bridge pier respect to Sa (1.4 T1, 5%)

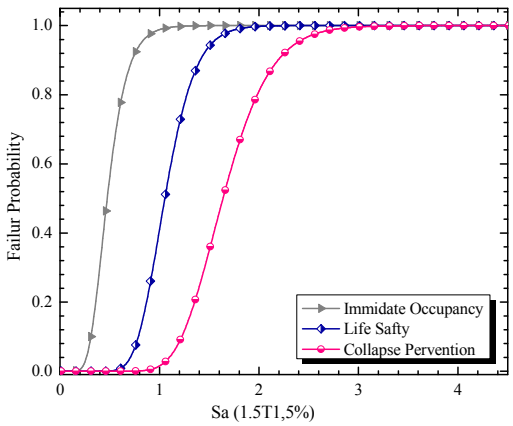

Fig. 57 Fragility curves of the bridge pier respect to Sa (1.5 T1, 5%)

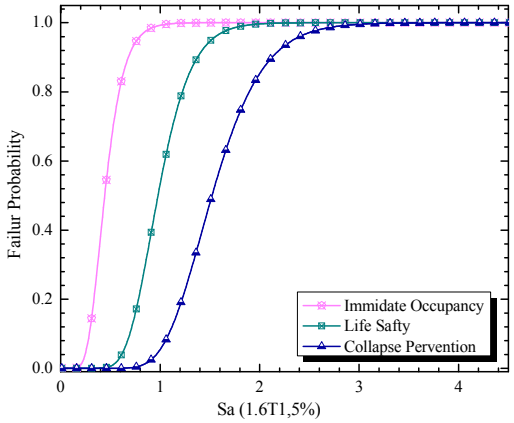

Fig. 58 Fragility curves of the bridge pier respect to Sa (1.6 T1, 5%)

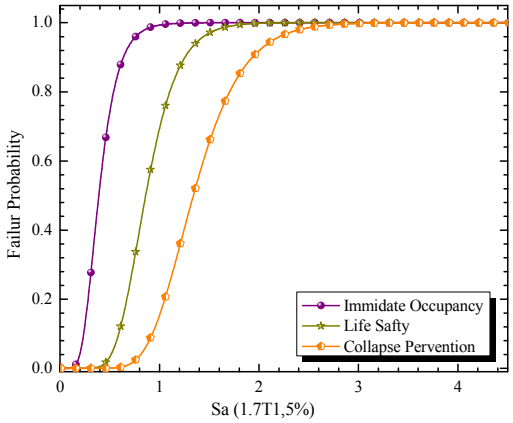

Fig. 59 Fragility curves of the bridge pier respect to Sa (1.7 T1, 5%)

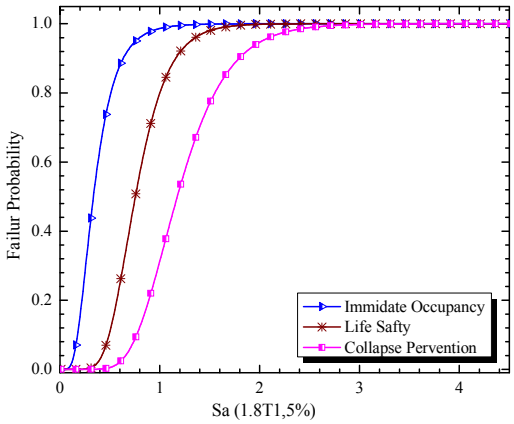

Fig. 60 Fragility curves of the bridge pier respect to Sa (1.8 T1, 5%)

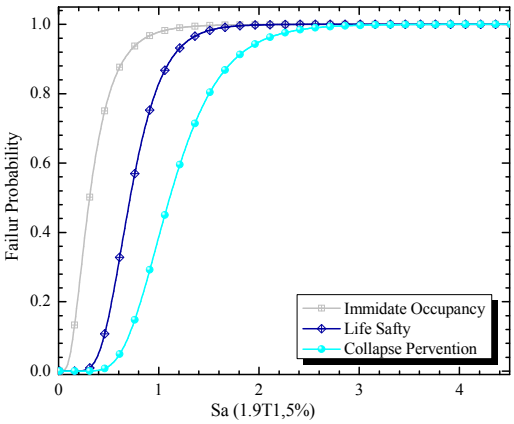

Fig. 61 Fragility curves of the bridge pier respect to Sa (1.9 T1, 5%)

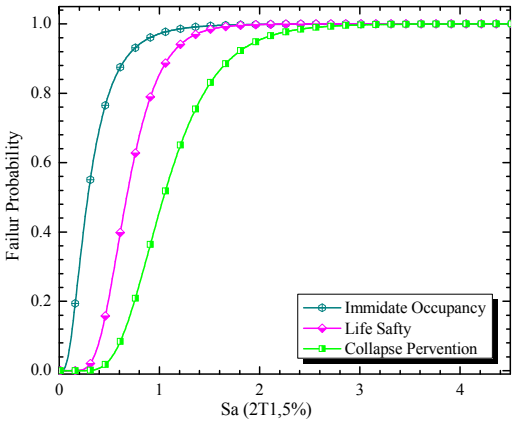

Fig. 62 Fragility curves of the bridge pier respect to Sa (2 T1, 5%)

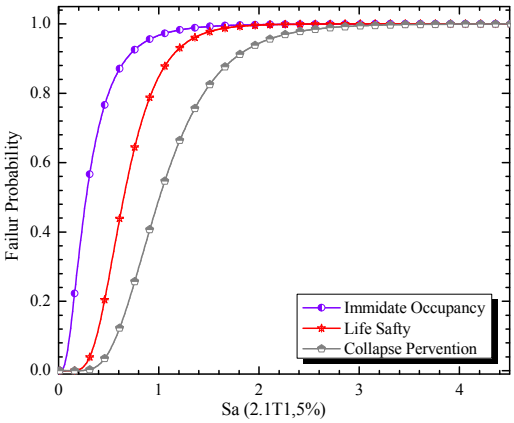

Fig. 63 Fragility curves of the bridge pier respect to Sa (2.1 T1, 5%)

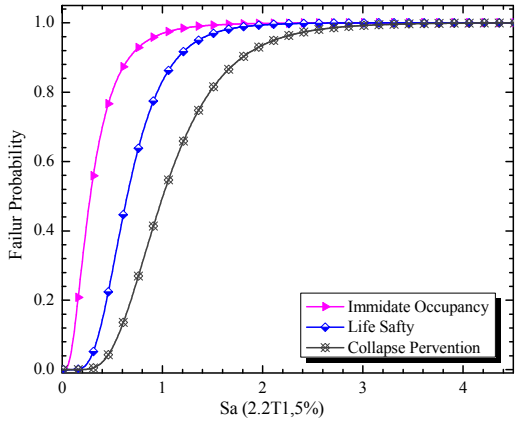

Fig. 64 Fragility curves of the bridge pier respect to Sa (2.2 T1, 5%)

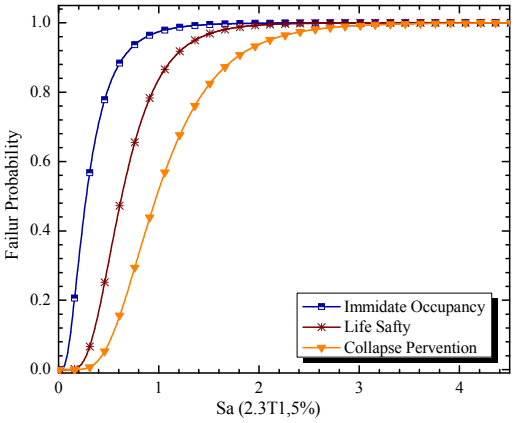

Fig. 65 Fragility curves of the bridge pier respect to Sa (2.3 T1, 5%)

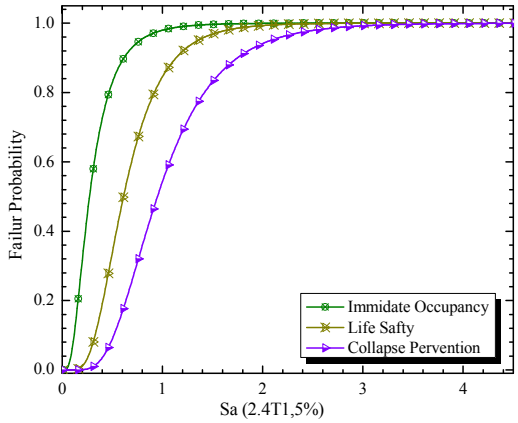

Fig. 66 Fragility curves of the bridge pier respect to Sa (2.4 T1, 5%)

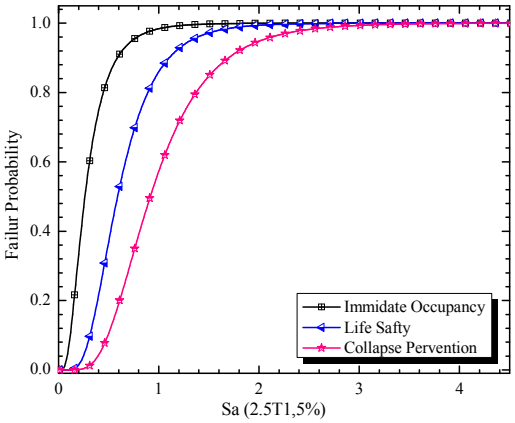

Fig. 67 Fragility curves of the bridge pier respect to Sa (2.5 T1, 5%)

6. Conclusions

In this paper, a detailed three dimensional bridge is defined and verified completely and it has been tried to achieve its analytical seismic fragility curves of straight three span concrete girder bridges. A total 20 suit records were selected and the incremental dynamic analysis was applied to the bridge. The results show that the selection of the records has a great effect on the response of the structures. The signification of the selecting an appropriate intensity measures and the response sensitivity was studied by considering a different range of Sa from Sa (0.05T1, 5%) to Sa (2.5T1, 5%). Their efficiency and practically of them were studied completely and compared. A critical range of Sa (Ti, 5%) was obtained by sensitive analysis on nonlinear time history data. The results show that that Sa (1.1T1, 5%) and Sa (1.2T1, 5%) are efficient enough and some spectral intensity measure are more practical than PGA but finally the Sa (1.2T1, 5%) is more proficient and it is followed by Sa (1.1T1, 5%) and Sa (1.5T1, 5%) than the other intensity measures related to the sensitive analysis. It has been indicated that through the sensitive analysis on the period of the

structure, selecting an appropriate range of Sa (Ti, 5%), can reduce the dispersion a lot and lead us to a more accurate fragility curve.

References

Agency, F.E.M. (2009), Quantification of Building Seismic Performance Factors, FEMA P695; Washington, D.C., USA.

Banerjee, S. and Shinozuka, M. (2008), "Mechanistic quantification of RC bridge damage states under earthquake through fragility analysis", *Probabilist. Eng. Mech.*, **23**(1), 12-22.

Basöz, N.I. and Kiremidjian, A.S. (1998), "Evaluation of bridge damage data from the Loma Prieta and Northridge", Technical Report MCEER; California Earthquakes.

Choi, E. (2002), Seismic Analysis and Retrofit of Mid-America Bridges. Dissertation, Department of Civil and Environmental Engineering, Georgia Institute of Technology, Atlanta, GA, USA.

Cimerallo, G.P., Reinhorn, A.M. and Bruneau, M. (2010), "Framework for analytical quantification of disaster resilience", *Eng. Struct.*, **32**(11), 3639-3649.

Cornell, A.C., Jalayer, F. and Hamburger, R.O. (2002), "Probabilistic basis for 2000 SAC federal emergency management agency steel moment frame guidelines", *J. Struct. Eng.*, **128**(4), 526-532.

Deepu, S.P., Prajapat, K. and Ray-Chaudhuri, S. (2014), "Seismic vulnerability of skew bridges under bi-directional ground motions", *Eng. Struct.*, **71**(9), 150-160.

Eads, L., Miranda, E., Krawinkler, H. and Lignos, D. (2013), "An efficient method for estimating the collapse risk of structures in seismic regions", *Earthq. Eng. Struct. Dyn.*, **42**(1), 25-41.

FEMA (2003), HAZUS-MH MR1: Technical Manual; Federal Emergency Management Agency Washington, D.C., USA.

Hwang, H. and Huo, J.R. (1998), "Probabilistic seismic damage assessment of highway bridges", *Proceedings of the Sixth U.S. National Conference on Earthquake Engineering*, Seattle, WA, USA, May-June; Earthquake Engineering Research Institute, Oakland, CA, USA. [on CD-ROM]

Hwang, H., Liu, J. and Chiu, Y. (2001), "Seismic fragility analysis of highway bridges", Technical Report; Center for Earthquake Research and Information, University of Memphis, Memphis, TN, USA.

Kameshwar, S. and Padgett, J.E. (2014), "Multi-hazard risk assessment of highway bridges subjected to earthquake and hurricane hazards", *Eng. Struct.*, **78**(11), 154-166.

Kaviani, P. (2011), "Performance-based seismic assessment of skewed bidges", Ph.D. Dissertation; University of California – Irvine, Irvine, CA, USA.

Karim, K.R. and Yamazaki, F. (2003), "A simplified method of constructing fragility curves for highway bridges", *Earthq. Eng. Struct. Dyn.*, **32**(10), 1603-1622.

Mackie, K.R., Wong, J.M. and Stojadinović, B. (2010), "Post-earthquake bridge repair cost and repair time estimation methodology", *Earthq. Eng. Struct. Dyn.*, **39**(3), 281-301.

Mander, J.B. and Basöz, N. (1999), "Seismic fragility curve theory for highway bridges", *Proceedings of the 5th U.S. Conference on Lifeline Earthquake Engineering*, Seattle, WA, USA, August, pp. 31-40.

Monti, G. and Nistico, N. (2002), "Simple probability-based assessment of bridges under scenario earthquakes", *J. Bridge Eng.*, **7**(2), 104-114.

Monti, G., Nisticò, N. and Santini, S. (2001), "Design of FRP jackets for upgrade of circular bridge piers", *J. Compos. Construct.*, **5**(2), 94-101.

Nielson, G.B. (2005), "Analytical fragility curves for highway bridges in moderate seismic zones", Georgia Institute of Technology; in partial requirement for the requirement for Doctor of Philosophy.

Padgett, J.E., Nielson, B.G. and DesRoches, R. (2008), "Selection of optimal intensity measures in probabilistic seismic demand models of highway bridge portfolios", *Earthq. Eng. Struct. Dyn.*, **37**(5), 711-725.

Padgett, J.E., Dennemann, K. and Ghosh, J. (2010), "Risk-based seismic life-cycle cost- benefit (LCC-B) analysis for bridge retrofit assessment", *Struct. Safe.*, **32**(3), 165-173.

Pan, Y., Agrawal, A.K., Ghosn, M. and Alampalli, S. (2010), "Seismic fragility of multispan simply supported

steel highway bridges in New York State. II: Fragility analysis, fragility curves, and fragility surfaces", *J. Bridge Eng*., **15**(5), 462-472.
Ramanathan, K.N. (2012), "Next generation seismic fragility curves for California bridges incorporating the evolution in seismic design philosophy", Georgia Institute of Technology; in partial requirement for the requirement for Doctor of Philosophy.
Rix, G. and Fernandez-Leon, J. (2004), *Synthetic Ground Motions for Memphis*, *TN*, *USA*.
Æ http://www. ce.gatech.edu/research/mae_ground_motions
Shinozuka, M., Feng, M.Q., Kim, H.-K. and Kim, S.-H. (2000a), Nonlinear static procedure for fragility curve development", *J. Eng. Mech*., **126**(12), 1287-1295.
Shinozuka, M., Feng, M.Q., Lee, J. and Naganuma, T. (2000b), "Statistical analysis of fragility curves", *J. Eng. Mech*., **126**(12), 1224-1231.
Sung, Y.-C. and Su, C.-K. (2011), "Time-dependent seismic fragility curves on optimal retrofitting of neutralised reinforced concrete bridges", *Struct. Infrastruct. Eng*., **7**(10), 797-805.
Tavares, D.H., Padgett, J.E. and Paultre, P. (2012), "Fragility curves of typical as-built highway bridges in eastern Canada", *Eng. Struct*. , **40**(9), 107-118.
Wright, T., DesRoches, R. and Padgett, J.E. (2011), "Bridge seismic retrofitting practices in the central and Southeastern United States", *J. Bridge Eng*., **16**(1), 82-92.
Yamazaki, F., Motomura, H. and Hamada, T. (2000), "Damage assessment of expressway networks in Japan based on seismic monitoring", *Proceedings of the 12th World Conference on Earthquake Engineering*, Auckland, New Zealand, January-February.
Yi, J.-H., Kim, S.-H. and Kushiyama, S. (2007), "PDF interpolation technique for seismic fragility analysis of bridges", *Eng. Struct*., **29**(7), 1312-1322.

CC